Study of the high-pressure phase behaviour of CO_2+n-alkane mixtures using the SAFT-VR approach with transferable parameters

F. J. Blas[1] and A. Galindo[2,*]

1 *Departamento de Física Aplicada e Ingeniería Eléctrica, Escuela Politécnica Superior, Universidad de Huelva, 21819 La Rábida, Huelva, Spain.*

2 *Department of Chemical Engineering and Chemical Technology, Imperial College of Science, Technology, and Medicine, Prince Consort Road, London SW7 2BY.*

* corresponding author: a.galindo@ic.ac.uk

Abstract

The statistical associating fluid theory for potentials of variable range (SAFT-VR) is used to examine the phase behaviour in the CO_2+n-alkane homologous series. A unique set of transferable parameters for the unlike interactions are used which allow the prediction of the phase behaviour of different members of the series with little experimental data. A change in phase behaviour from type II in the van Konynenburg scheme (continuous gas-liquid critical line and liquid-liquid immiscibility at low temperatures) for CO_2+n-dodecane, to IV (discontinuous gas-liquid critical line and liquid-liquid immiscibility) for CO_2+n-tridecane, and to III (continuous transition from gas-liquid to liquid-liquid critical behaviour) for CO_2+n-tetradecane is observed in agreement with experimental data.

1. Introduction

Supercritical carbon dioxide (CO_2) is an useful replacement for organic solvents. It is non-flammable, essentially non-toxic, and the least expensive solvent after water. It has a critical temperature near ambient temperature (T_c=304.21 K[1], as compared to the critical temperature of water which is 647 K[2]), a reasonable critical pressure (p_c = 7.383 MPa[1], while that of water is 22 MPa[2]), and a critical density higher than that of most other supercritical solvents. It has become essential in supercritical extraction applications, and as media for supercritical polymerisation processes. CO_2 has no dipole moment due to the symmetry of the molecule, but it presents a significant quadrupole moment. Even at very high pressures CO_2 has far weaker van der Waals forces that those of hydrocarbons, making it more like a fluorocarbon. CO_2 is miscible with the shorter hydrocarbons, providing the pressure is sufficiently high, but it remains immiscible with polymers such as polyethlyene even for extreme pressures. Further interest in mixtures of CO_2 + n-alkanes arises from studies of the continuity of fluid phase behaviour in mixtures. Following the classification for binary mixtures given by Scott and van Konynenburg[3], transitions from type I to type II, IV, and finally III, are seen in the homologous series of CO_2 + n-alkanes as the chainlength of the hydrocarbon increases[4,5]. Mixtures of CO_2 with n-alkanes shorter than, and up to n-hexane (n-C_6H_{14}), exhibit type I phase behaviour; a continuous gas-liquid critical curve is observed between the critical points of the pure components, while the liquid phase is fully miscible (liquid-liquid separation is pre-empted by the solidification of CO_2[5] at T=216.55 K[1]). For mixtures of CO_2 with longer n-alkanes two immiscible liquid phases are present at low temperatures. In terms of the pT phase diagram a continuous gas-liquid critical line joins the critical points of the two pure components, while a liquid-liquid critical line is found at low temperatures (this diagram corresponds to type II phase behaviour). The liquid-liquid critical line merges with a three phase (liquid-liquid-vapour) line at an upper critical end point (UCEP). The UCEP for the CO_2 + n-heptane (n-C_7H_{16}) system is observed at T_{UCEP}=222.60 K and p_{UCEP}=0.656 MPa[5]. Similarly, mixtures of CO_2 + n-octane (n-C_8H_{18}), n-nonane(n-C_9H_{20}), n-decane(n-$C_{10}H_{22}$), n-undecane (n-$C_{11}H_{24}$) and n-dodecane (n-$C_{12}H_{26}$) are seen to exhibit phase behaviour of type II, although as expected, the extent of immiscibility increases as the chainlength of the n-alkane increases. In the case of n-dodecane the UCEP is found at T_{UCEP} = 267.31 K and p_{UCEP} =2.0326 MPa[5]. Particularly interesting is the transition observed for CO_2 + n-tridecane (n-$C_{13}H_{28}$), which exhibits a phase behaviour of type IV[6]. In

this system two immiscible liquid phases are observed at low temperatures, and a three-phase line starting at very low temperatures and pressures and finishing at an UCEP at T_{UCEP} =278.95 K and p_{UCEP}=3.985 MPa is observed. However, close to the critical point of CO_2 a second region of immiscibility is found bounded below by a lower critical end point (T_{LCEP}=310.75 K and p_{LECP}=8.221 MPa) and above by a second UCEP (T_{UCEP}=314.01 K and p_{UCEP}=8.831 MPa). As a result, the vapour-liquid critical line is discontinuous in this system, running from the critical point of n-$C_{13}H_{28}$ to the LECP, and from the UCEP to the critical point of CO_2. The lower and upper critical end points close to the CO_2 critical region merge quickly into each other giving rise to type III phase behaviour as the extent of immiscibility increases in the mixture; i.e., as the n-alkane chainlength increases. A transition from type IV to type III phase behaviour is observed for CO2 + n-tetradecane (n-$C_{14}H_{30}$)[5], where a continuous change from gas-liquid to liquid-liquid immiscibility is observed. The gas-liquid critical line starting at the critical point of the less volatile component (the n-alkane) turns continuously into a liquid-liquid critical line at lower temperatures. A second short critical line is observed from the critical point of CO_2 to an UECP where the three phase line also finishes. The system exhibits a single UCEP at T_{UCEP}=311.14 K and p_{UCEP}=8.369 MPa.

The main objective of this work, which forms part of a larger study involving mixtures of CO_2, is to investigate the delicate transition occurring between the mixtures of CO_2 + n-$C_{12}H_{26}$ (type II), CO_2 + n-$C_{13}H_{28}$ (type IV) and CO2 + n-$C_{14}H_{30}$ (type IV). We use the statistical associating fluid theory for potentials of variable range (SAFT-VR) to predict the phase behaviour of the CO_2 + n-alkane homologous series using only one set of transferable parameters. Before presenting the results, however, it is useful to give a short overview of the theoretical approach.

2. Models and theory.

The statistical associating fluid theory (SAFT)[7] provides a very versatile and accurate tool to study complex fluid phase behaviour. The approach stems form the thermodynamic perturbation theory of Wertheim[8,9], which gives rigorous expressions for the densities and free energy contributions of associating chain fluids. The SAFT approach was put in the form of an equation of state for fluids of associating Lennard-Jones chain molecules in its first version[7] using a hard-sphere fluid is used as reference, and the long-range attractive forces treated with the expansion of Cotterman *et al.*[10] for the Lennard-Jones potential. More recently, a number of modifications and extensions have been presented in which the structure of the reference fluid is treated in more detail[11]. In particular, in the SAFT-VR approach[12] an attractive potential of variable range and arbitrary shape is considered; the square-well is the most commonly used. The introduction of an extra non-conformal parameter λ which describes the range of the potential gives this approach an added advantage in dealing with polar interactions in an effective way.

In terms of the free energy of a mixture of associating chain molecules the free energy in the SAFT-VR approach can be written in four separate terms as[12]

$$\frac{A}{NkT} = \frac{A^{IDEAL}}{NkT} + \frac{A^{MONO.}}{NkT} + \frac{A^{CHAIN}}{NkT} + \frac{A^{ASSOC.}}{NkT}$$

where N is the number of chain molecules, k is Boltzmann's constant, and T is the temperature. A^{IDEAL} is the ideal free energy of the mixture, $A^{MONO.}$ is the residual contribution due to monomer-monomer interactions, A^{CHAIN} is the contribution due to chain formation, and $A^{ASSOC.}$ Accounts for the association. In the SAFT-VR approach the monomer segments are modelled with an arbitrary attractive potential; in this work we use square-well potentials of depth ε_i and

range $\lambda_{i,}$, where i indicates the component. The contribution to the free energy due to the monomer-monomer interactions is obtained from a high-temperature perturbation expansion up to second order so that [12]

$$\frac{A^{MONO}}{NkT} = \sum_i (x_i m_i)\left(a^{HS} + \frac{1}{kT} a_1 + \frac{1}{(kT)^2} a_2 \right),$$

where x_i is the mole fraction, m_i is the number of segments in a molecule of component i, a^{HS} is the residual hard-sphere free energy, a_1 the mean attractive energy, and a_2 the fluctuation term of the mixture. The contribution to the free energy due to chain formation in a mixture is given by[13]

$$\frac{A^{CHAIN}}{NkT} = -\sum_i x_i (m_i - 1) \ln y^{SW}(\sigma_{ii}),$$

where $y(\sigma_{ii})$ is the cavity distribution function of the reference monomer fluid at contact. The free energy due to association is given by

$$\frac{A^{ASSOC.}}{NkT} = \sum_{i=1}^{n} x_i \left[\sum_{a=1}^{s_i} \left(\ln X_{a,i} - \frac{X_{a,i}}{2} \right) + \frac{s_i}{2} \right],$$

where the first sum is over the number of components, and $X_{a,i}$ is the fraction of molecules of type i not bonded at site a given as

$$X_{a,i} = \frac{1}{1 + \rho \sum_{j=1}^{n} \sum_{b=1}^{s_j} x_j X_{b,j} \Delta_{a,b,i,j}},$$

where $\Delta_{a,b,i,j}$ is a parameter describing the interaction between sites a and b in molecules i and j . In this work we are interested in mixtures involving two non-associating components, so that $\Delta_{a,b,i,j} = 0$ and hence $A^{ASSOC.}/NkT = 0$.

We model the CO_2 molecules as non-associating and non-spherical. In several occasions associating sites have been used in order to model polar molecules in an effective way; a two-site model incorporates chain aggregates of similar conformation to the favourable head-to-tail dipole-dipole interaction. CO_2 has no permanent dipole moment due to the symmetrical linear shape of the molecule, but, as mentioned in the introduction, it has a considerable quadrupole moment. We have not, however introduced quadrupolar interactions explicitely in this work. Instead the attractive dispersion interactions and the quadrupole are treated in an effective way via a square-well potential of depth ε_1 of adjustable range λ_1. The non-spherical shape of both the CO_2 and the n-alkane molecules is taken into account explicitely in the SAFT approach, so that m_1 spherical segments of hard-core diameter σ_1 form a CO_2 molecule, and m_2 spherical segments of hard-core diameter σ_2 form an n-alkane molecule. The long-range dispersion interactions for the n-alkane molecule are modelled using square-well potentials of depth ε_2 and range λ_2.

3. Results and discussion.

In order to compare with real systems, we have optimised the intermolecular potential parameters m, σ, ε and λ of the pure components using experimental vapour pressures and saturated densities for each substance (see table 1). In particular the vapour pressures and coexistence densities for CO_2[1] are compared with the SAFT-VR calculations in figure 1. Good agreement is obtained, although the critical temperature and pressure are overpredicted as characteristic

of a classical equation of state. In order to give a better description of the critical region we rescale the conformal parameters σ and ε to the experimental critical points. It is clear from the figure that the improvement of the critical point results in a detriment to the saturated liquid densities; at this point in time we are particularly interested in examining the critical curves of the mixtures in order to characterise the transitions in type of phase behaviour described in the introduction, and hence use the rescaled parameters σ_c and ε_c.

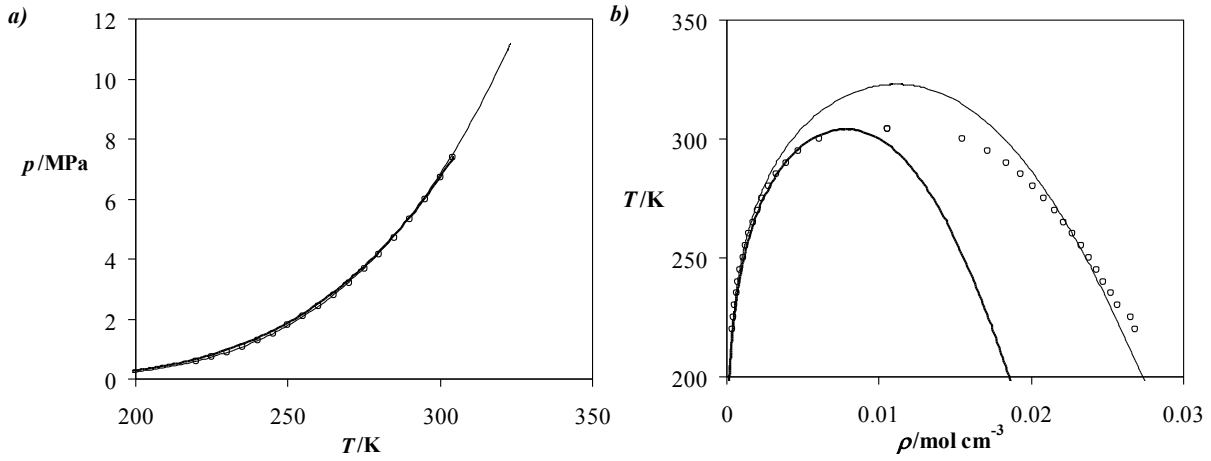

Figure 1. *a*) Vapour pressures and *b*) saturated liquid coexistence densities for CO_2 compared with SAFT-VR calculations. The thin curve corresponds to the SAFT-VR calculation with the optimised parameters, and the bold curve to the calculations using the parameters rescaled to the critical point (see text and table 1 for The symbols correspond to the experimental data.

The optimised parameters for the n-alkane series have already been presented elsewhere together with linear relationships for σ, ε, and λ[14]. As in previous works, a simple empirical relationship is also used to relate the number of carbons in the n-alkane chain and the number of spherical segments m in the model: $m_2 = (C\text{-}1)/3 + 1$. In our calculations we use λ_2 as obtained from the relationship $m_2\lambda_2 = 0.03900\ MW_2 + 0.873$[14], while the conformal

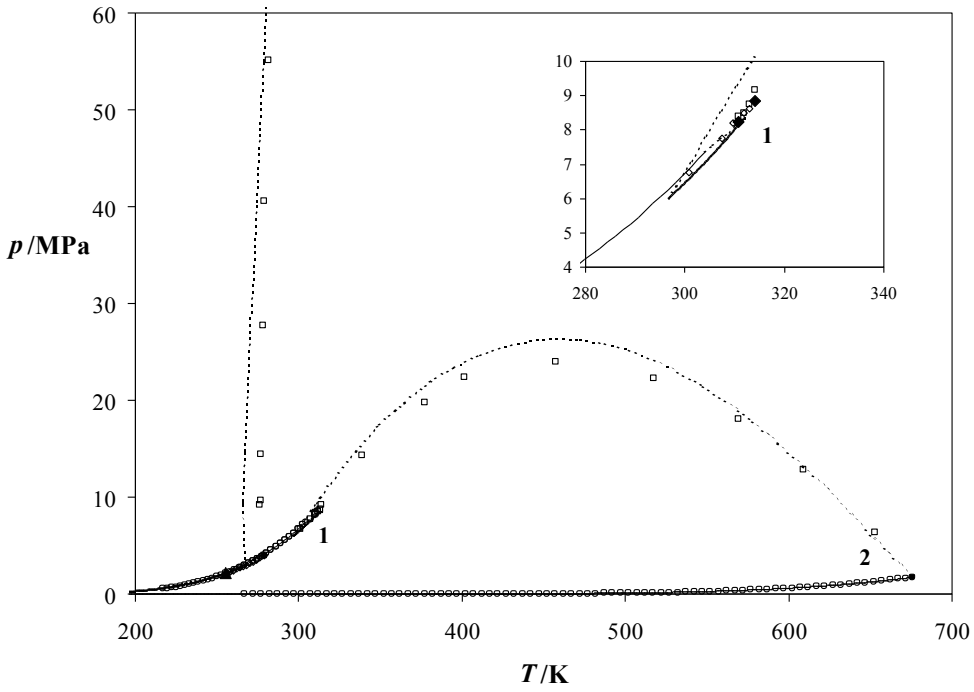

Figure 2. *pT* projection of the *pTx* phase diagram for CO_2 (1) + n-tridecane (2) compared with the SAFT-VR predictions. The thin solid curves correspond to the calculated pure component vapour pressures, the bold solid curves to the three phase lines and the dashed curves to critical lines. The open circles correspond to the experimental pure vapour pressures, the filled circles to pure component critical points, the open squares to mixture critical points, the diamonds to lower and upper critical end points and the filled triangle to the solid-liquid-liquid-vapour four-phase point.

parameters σ_2 and ε_2 are rescaled in order to obtain the best description of the critical point in each case (see Table 1).

In terms of the mixtures, two unlike intermolecular parameters ε_{12} and λ_{12} need to be determined. Since the classic Lorentz-Berthelot combining rule is not adequate for these complex systems, we readjust ε_{12} and λ_{12} defining two adjustable mixture parameters ξ=0.88 and γ=0.989 (where $\varepsilon_{12} = \xi\ (\varepsilon_1\ \varepsilon_2)^{1/2}$ and $\lambda_{12} = \gamma\ (\lambda_1\ \sigma_1 + \lambda_2\ \sigma_2)\ /\ (\sigma_1 + \sigma_2)$) to ensure that the mixture of CO_2 + n-$C_{13}H_{28}$ mixture exhibits type IV phase behaviour (see figure 2). Using these unlike intermolecular parameters the phase behaviour of the CO_2 + n-$C_{13}H_{28}$ mixture is very well described by the theory. It is important to note that only one set of parameters is necessary in order to describe the phase behaviour of the mixture for the entire fluid range. Furthermore, as mentioned in the introduction, mixtures of CO_2 with n-alkanes exhibit characteristic transitions in the types of phase behaviour as the alkane chainlength changes. While the mixture of CO_2 + n-$C_{13}H_{28}$ exhibits type IV phase behaviour (discontinuous gas-liquid critical curve and liquid-liquid critical line at low temperature; see figure 2), the mixture of CO_2 + n-$C_{12}H_{26}$ exhibits type II phase behaviour (continuous gas-liquid critical line and liquid-liquid critical line at low temperature). The change in type of behaviour can be understood considering that the shorter n-$C_{12}H_{26}$ is more miscible in CO_2 than n-$C_{13}H_{28}$, and so the small region of immiscibility close to the critical point of CO_2 shrinks to disappear. In CO_2 + n-$C_{14}H_{30}$ mixture the greater degree of immiscibility results in type III phase behaviour (continuous gas-liquid to liquid-liquid critical line).

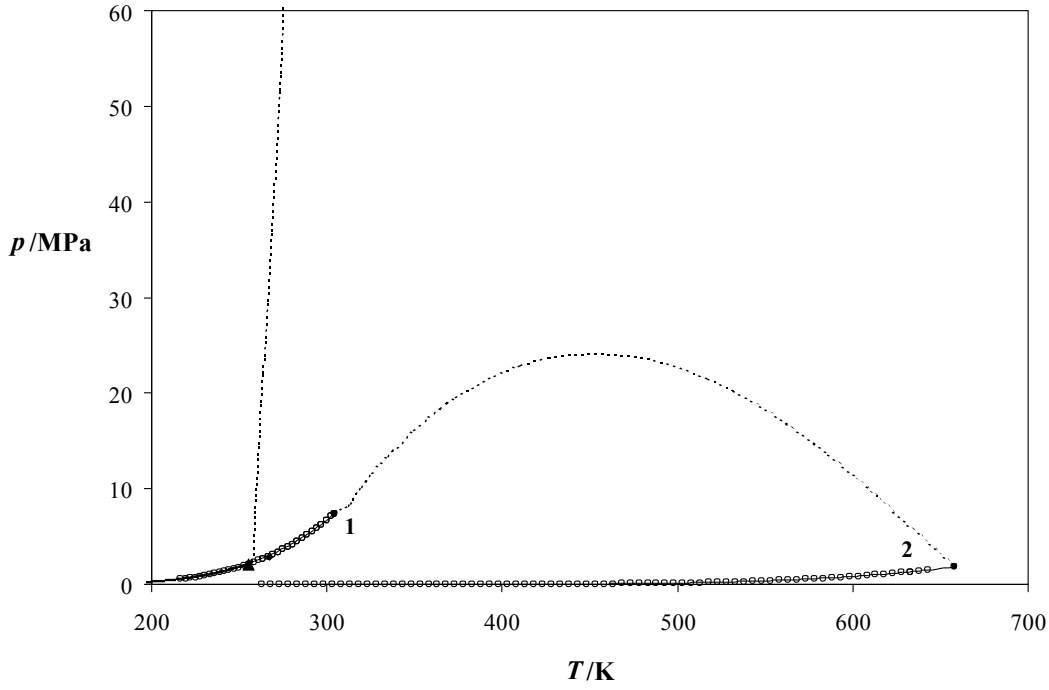

Figure 3. *pT* projection of the *pTx* phase diagram for CO_2 (1) + n-dodecane (2) compared with SAFT-VR predictions. The thin solid curves correspond to the calculated pure component vapour pressures, the bold solid curves to the three phase line and the dashed curves to the critical curves. The open circles correspond to the experimental pure component vapour pressures, the filled circles to the pure component critical points, the filled diamond to the upper critical end point, and the filled triangle to the solid-liquid-liquid-vapour four phase point.

We are able to describe these delicate changes with a unique set of transferable parameters (ξ=0.88 and γ=0.989). Clearly, the change chainlength for each of the n-alkanes is taken into account explicitly in the SAFT approach, as expected then, the extent of the attractive forces between CO_2 and the n-alkanes must be the similar for the members of the homologous series. This is especially true for the mixtures we study in this work where the end-effects of the CH_3 groups, which are seen in shorter n-alkanes, are less important. The predicted phase behaviour for CO_2 + n-dodecane is

shown in figure 3. The mixture exhibits type II phase behaviour as mentioned, and the calculations find very good agreement with the experiment. Using the same set of transferable parameters a mixture of CO_2 + n-tetradecane has been studied. The SAFT-VR approach predicts type III phase behaviour for this system, which is also in agreement with experimental data.

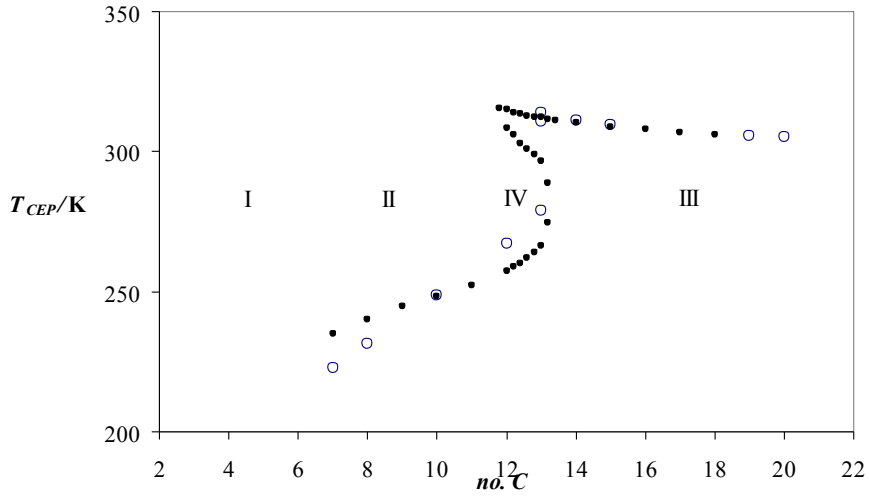

Figure 4. Temperature of the critical end points (CEP) for mixtures of CO_2 + n-alkanes compared with SAFT-VR predictions for increasing n-alkane chain length. The open circles correspond to the experimental data and filled circles to the calculations. The types of fluid phase behaviour, which can be determined from inspection of the critical end points are also indicated.

In figure 4 we summarise a global phase diagram for mixtures of CO_2 + n-alkanes presenting the critical end points (CEP) of the mixture. The critical end points delimit the regions of three-phase coexistence, and together with this the extent of liquid-liquid immiscibility. Mixtures of type I present no CEP (these are pre-empted by the appearance of the solid phases), mixtures of type II present one CEP at low temperature, while mixtures of type III present one CEP close to the critical point of the more volatile component (CO_2 in this case). The transition from type II to type III occurs via type IV phase behaviour, which presents three CEP which are the limits of the two three-phase lines (one starting at very low temperatures and pressures at a four-phase solid-liquid-liquid-gas point and finishing at an UCEP well below the critical point of the more volatile component, and a second, short three phase line with lower and upper critical end points which are close to the critical point of the more volatile component). In figure 4 the experimental critical end points for CO_2 + n-alkane mixtures from n-heptane to n-eicosane are compared with the SAFT-VR calculations. As before, the unique set of unlike parameters ξ=0.88 and γ=0.989 is used for all the systems studied. Clearly, the SAFT-VR approach gives a good description of the phase behaviour of the homologous series. In a following study we will examine in more detail the phase behaviour of these mixtures considering also the coexistence compositions.

Table1. Optimised SAFT-VR square-well intermolecular potential parameters. m is the number of spherical segments in the model, s is the hard-core diameter, and e and l are the depth and range of the square-well. The subscript c indicates that the parameters have been rescaled to the experimental critical point, and $T_c^*=kT_c/\varepsilon$ and $p_c^*=pb^2/\varepsilon$, where $\alpha=2\pi/3\sigma^3\varepsilon(\lambda^3-1)$ and $b=\pi/6\sigma^3$ are the reduced critical temperature and pressure.

	m	σ/Å	ε/k (K)	λ	T_c^*	$p_c^* 10^3$	σ_c/Å	ε_c/k (K)
CO2	2.0	2.7864	179.27	1.5257	0.18146	5.1528	3.1364	168.89
n-C12	4.667	3.9619	247.42	1.6077	0.22533	2.3460	4.6271	231.44
n-C13	5.0	3.9671	248.70	1.6098	0.22919	2.1932	4.6260	232.41
n-C14	5.333	3.9716	249.82	1.6116	0.23276	2.0567	4.6340	233.41

4. List of symbols

T	temperature
p	pressure
A	Hemholtz free energy per molecule
a	Hemholtz free enerfy per segment
N	number of molecules
k	Boltzmann's constant
x_i	mole fraction of componet i
m	number of spherical segments
y	cavity distribution function
$X_{a,i}$	fraction of molecules of type i with not bonded at site a
s	total number of sites

Greek letters

σ	hard-core diameter
ρ	density
$\Delta_{a,b,i,j}$	association interaction parameter for sites a and b in molecules i and j
λ	square-well range
ε	square-well depth
ξ	unlike energy interaction parameter
γ	unlike square-well range interaction parameter
α	integrated energy paramter
b	hard-core volume

Subscripts

i,j	components
a,b	type of site

References

[1] N. B. Vargaftik, *'Table on Thermophysical Properties of Liquids and Gases'*, Hemisphere Publishing, New York, USA (1975).

[2] J. S. Rowlinson, and F. L. Swinton, *'Liquids and liquid mixtures',* 3rd. Ed., Butterworths, London (1981).

[3] R. L. Scott and P. H. van Konynenburg, Discuss. Faraday Soc., 49 (1970) 87; P. H. van Konynenburg, and R. L. Scott, Phylos. Trans. R. Soc. A., 298 (1980) 495.

[4] G. M. Schneider, J. Supercrit. Fluids, 13 (1998), 5.

[5] M. M. Miller, and K. D. Luks, Fluid Phase Equilib., 44 (1989), 295.

[6] R. Enick, G. D. Holder and B. I. Morsi, Fluid Phase Equilib., 22 (1985) 209.

[7] W. G. Chapman, K. E. Gubbins, G. Jackson, and M. Radosz, Fluid Phase Equilib., 51 (1989) 31; W. G. Chapman, K. E. Gubbins, G. Jackson, and M. Radosz, Ind. Eng. Chem. Res., 29 (1989) 1709.

[8] M. S. Wertheim, J. Stat. Phys., 35 (1984) 19; *ibid*., 35 (1984) 35.

[9] M. S. Wertheim, J. Stat. Phys., 42 (1986) 459; *ibid*., 42 (1984) 477.

[10] R. L. Cotterman, B. J. Schwartz, and J. M. Prausnitz, AIChE J., 32 (1986) 1787.

[11] E. A. Muller, and K. E. Gubbins, 'Equations of state for fluids and fluid mixtures', Chapter 12, Elsevier, Amsterdam (2000).

[12] A. Gil-Villegas, A. Galindo, P. J. Whitehead, S. J. Mills, G. Jackson, and A. N. Burgess, J. Chem. Phys., 106 (1997) 4268; A. Galindo, L. A. Davies, A. Gil-Villegas, and G. Jackson, Mol. Phys., 93 (1998) 241.

[13] W. G. Chapman, J. Chem. Phys., 93 (1990) 4299.

[14] C. McCabe, and G. Jackson, Phys. Chem. Chem. Phys., 1 (1999) 2057.